

which poses a computationally demanding numerical simulation (Yao and Anandarajah, 2003, Jaradat and Abdelaziz, 2019).

SIMPLIFIED PHYSICO-CHEMICAL CONTACT MODEL FOR COHESIVE SOILS

The analytical solution for the interparticle forces in cohesive soils adds a considerable computational time to the finite difference formulation of DEM simulations, especially when implementing the double layer repulsive force (Yao and Anandarajah, 2003). Therefore, we simplified the analytical solution by introducing linear springs to simulate van der Waals attractive and double layer repulsive forces. The main advantage of the simplified model is that it reproduces the net interparticle force acting between clay particles with a minimal error in the approximation while allowing the use of larger timesteps that reduce the computational time considerably. These advantages allow simulating more particles to represent cohesive assemblies effectively. The analytical versus the simplified solutions are presented in Figure 1. The simplified contact model and its computational efficiency are presented elsewhere (Jaradat and Abdelaziz, 2020).

VALIDATING THE NUMERICAL SIMULATIONS

The mathematical formulation of the interparticle forces acting between clay particles (Figure 1) was coded in a discrete element framework using the particle flow code in two, PFC2D (PFC2D, 2019). Clay particles are modelled as rigid clumps, with a particle size distribution similar to the kaolinite used in the experimental test (Figure 2) for validation. All particles were $0.06 \mu\text{m}$ in thickness; all other used parameters are listed in Table 1. These parameters were derived from the analytical solution force-displacement relationship in Figure 1 as reported in Jaradat and Abdelaziz (2020). To quantify the impact of fabric anisotropy on shear strength, simulations with different fabrics were carried out as discussed next.

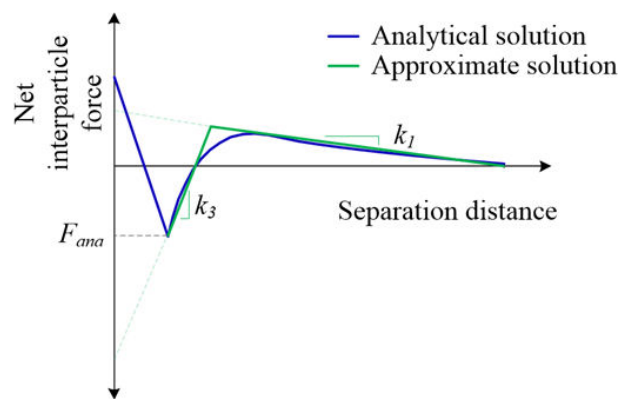


Figure 1. Simplified linear physico-chemical contact model adopted in this study.

Preparation of the numerical sample: Preparation of the numerical specimen mimicked the procedures used to prepare the bulk clay sample used in the experimental test. Within the DEM framework, 2,580 clay particles were first randomly generated in a $6.0 \times 20 \mu\text{m}$ smooth container. The model was then cycled to ensure that particles are not overlapping. After that, the interparticle forces were applied and the assembly was one-dimensionally (1-D) consolidated under 100 kPa vertical stress. After achieving the desired 1-D pressure, the assembly was

isotropically-consolidated under an effective pressure of 400 kPa. The consolidated numerical sample is shown in Figure 3. For all stages, equilibrium was ensured by solving for an average unbalanced force ratio (R), as defined by of 1×10^{-5} .

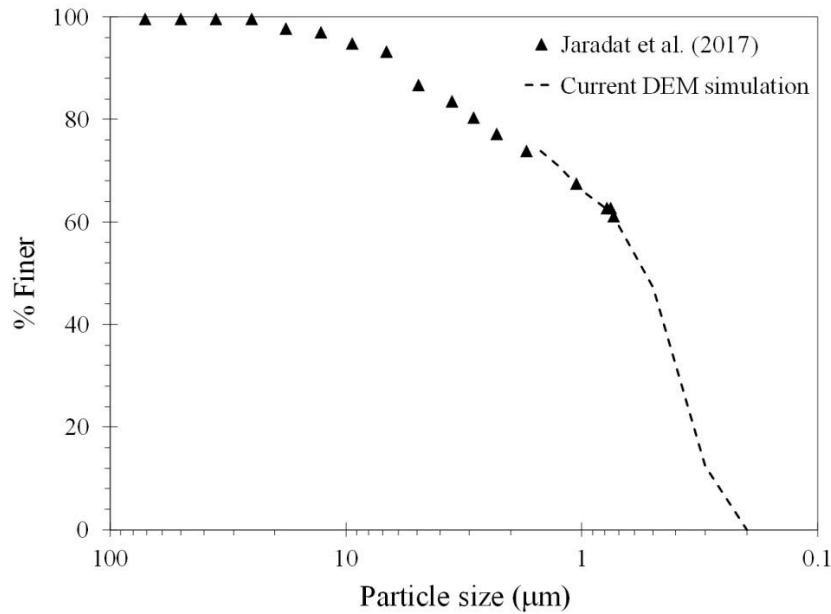


Figure 2. Particle size distribution of the numerical sample in this study.

Table 1. Parameters for the simplified model for the kaolinite-water electrolyte system.

Parameter	Value
Physico-chemical cut-off (d_p)	5.0 nm
Mechanical cut-of (d_m)	0.9 nm
Repulsive linear spring stiffness (k_1)	0.093 kN/m
Attractive linear spring stiffness (k_2)	2.96 kN/m
Mechanical spring stiffness ($k_n = k_s$)	1.5 kN/m
Mineral to mineral friction angle (ϕ')	10°

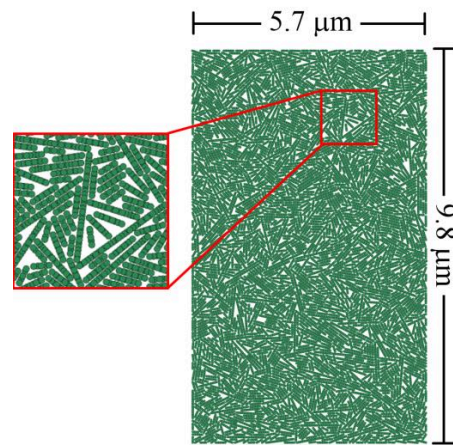


Figure 3. The consolidated numerical sample used in the current study.

Simulation of drained shearing: Upon achieving 400 kPa, drained shearing was initiated. In the experimental test, the rate of deviatoric loading (0.2%/hr) was selected according to ASTM D7181-11 to ensure no pore pressure buildup occurred during shearing. The lab test was carried out using a temperature-controlled triaxial cell modified from a conventional Trautwein triaxial system. The system and materials used, and sample preparation are described in detail by Jaradat and Abdelaziz (2020). In the DEM simulation, and since there is no pore pressure development, the rate at which the sample was sheared was chosen to keep the unbalanced force ratio as low as 1×10^{-5} , which was achieved by moving the top boundary wall downward at $0.001 \mu\text{m}/\text{sec}$. The stress-strain curve of the numerical model, as well as the volumetric strains during shearing are plotted against the experimental results in Figure 4. The results of the numerical model are in good agreement with the experimental results indicating the validity of the numerical model (Jaradat and Abdelaziz, 2020).

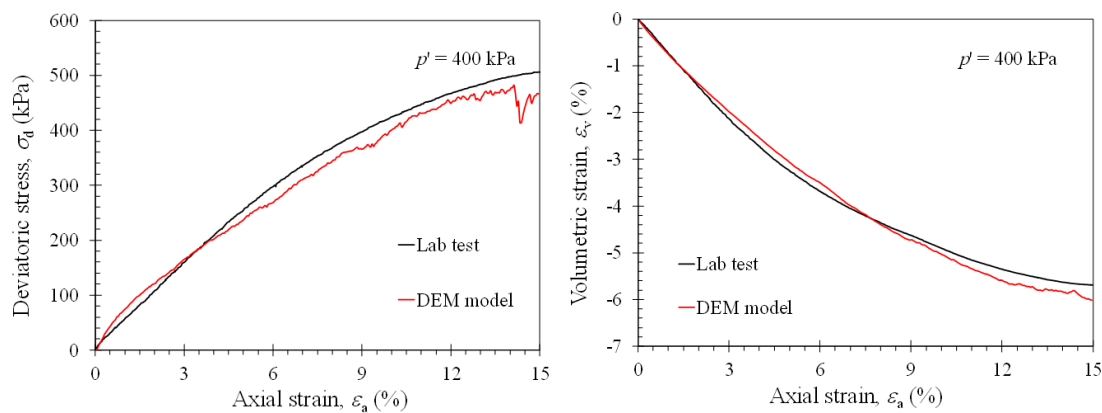


Figure 4. DEM model validation against an experimental lab test.

IMPACT OF FABRIC ANISOTROPY

Through DEM, different specimen fabrics can be obtained by different sample preparation methods (Yimsiri and Soga 2010). It is well-established that 1-D consolidation of clays creates a preferred particle orientation that is perpendicular to the loading direction (Jaradat et al. 2017); in other words, 1-D consolidation facilitates creating a dispersed fabric. The effect of the fabric anisotropy on the drained shearing response was assessed by performing three DEM simulations at the same mean effective stress (σ'_3) of 300 kPa, but at different fabrics. Different specimen fabrics were generated by applying different 1-D consolidation stress (p') during specimen preparation prior to shearing. Specimen “A” was 1-D consolidated under 200 kPa, then isotropically consolidated to 300 kPa; specimen “B” was 1-D consolidated under 50 kPa, then isotropically consolidated to 300 kPa. Finally, specimen “C” was isotropically consolidated to 300 kPa from slurry, i.e. 1-D consolidation stress of 0.0 kPa. All specimens were sheared under a constant mean effective stress (i.e. drained shearing) of 300 kPa, at a $0.001 \mu\text{m}/\text{sec}$ shearing rate as discussed previously. All specimens were sheared to 15% axial strain at which the numerical models were terminated. Figure 5 presents the shearing results for these three specimens. It is clear in Figure 5 that the specimen prepared at the highest 1-D consolidation (200 kPa) showed higher drained shear strength and more tendency to change volume during shearing. These results are discussed in light of the effective stress concept and specimen anisotropy in the next section.

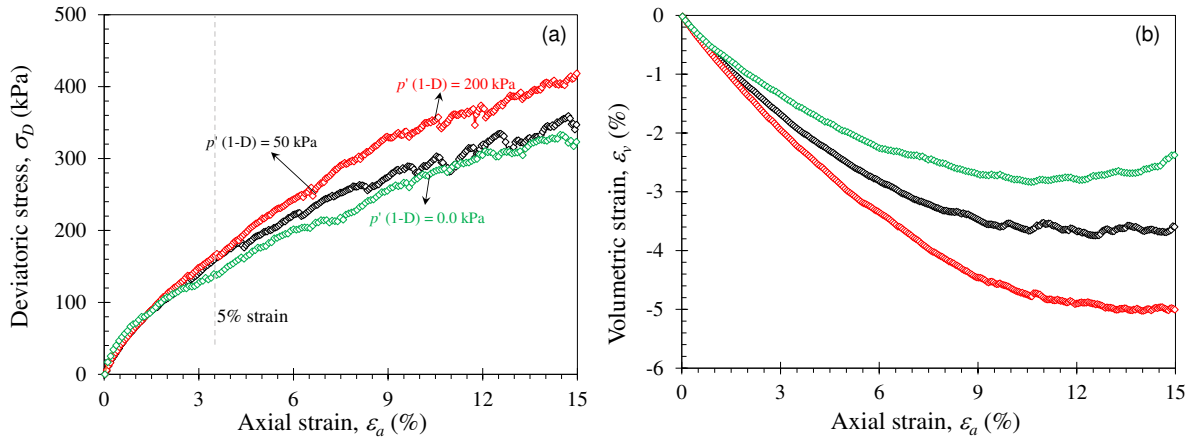


Figure 5. DEM simulation of drained shearing response of kaolinite samples prepared first at 0, 50, and 200 kPa 1-D axial stresses (p'), then sheared at the same mean effective stress of 300 kPa.

RESULTS AND DISCUSSIONS

Figure 5 presented the drained shearing response of the three clay kaolinite specimens. The shear strength and the 5% secant modulus increased with increasing the 1-D consolidation stress used during sample preparation prior to shearing. The drained shear strength and the 5% secant modulus of the sample prepared at 200 kPa 1-D stress are about 415 kPa and 4320 kPa, respectively, while the sample that was isotropically consolidation to 300 kPa had a 333 kPa drained shear strength and a 3550 kPa 5% secant modulus. The sample prepared at 50 kPa had a shear strength and stiffness values in between those of the two samples. These results are explained by looking at the distribution of the particle orientation prior shearing as follows.

Figure 6 presents the distribution of the particles' orientation of the three kaolinite specimens before shearing. The orientation of a particle is inferred from the inclination of its major local axis (α) from the horizontal axis in the 2D domain. It is shown that the sample prepared at 200 kPa has more particles (9.4%) oriented horizontally ($\alpha = 0.0^\circ$), while 3.3% particles were vertical ($\alpha = 90^\circ$). On the other hand, the sample with zero 1-D consolidation stress has more particles oriented vertically (7.7%), while 5.3% of the particles were horizontal. This implies that the specimen with a dispersed fabric is stronger and stiffer than the specimen with a flocculated fabric. Similar conclusions were drawn experimentally using true triaxial testing (Parshant and Penumadu, 2007).

Interestingly, the sample prepared at 1-D consolidation stress of 50 kPa has a preferred particle orientation that is close to that prepared at 1-D consolidation stress of 200 kPa as shown in Figure 6. Still, the sample prepared at 1-D consolidation stress of 200 kPa has more particles oriented horizontally and less particles oriented vertically compared to the 50 kPa sample, which is the reason for the noticed stronger and stiffer response of the former sample (Figure 5). This indicated that a small 1-D consolidation stress results in a preferred horizontal particles orientation or a dispersed fabric.

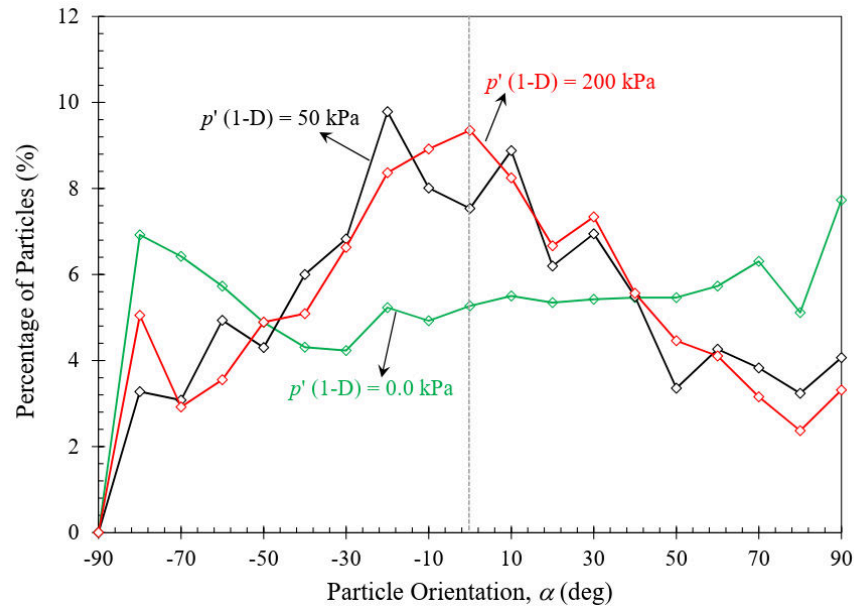


Figure 6. Distribution of the particles' orientation for the three numerical kaolinite samples before drained shearing.

The concept of the true effective stress (Santamarina and Fam, 1995) is adopted here to further explain the difference in shear behavior obtained numerically for flocculated and dispersed fabrics. Mathematically, the true effective stress, σ_m , is given by Eq. (1).

$$\sigma_m = \sigma_{tot} - u_0 - (R - A) \quad (1)$$

where σ_{tot} is the total stress, u_0 is the pore-fluid pressure, R is the interparticle repulsion, and A is the interparticle attraction. Eq. (1) suggests that cohesive soils behavior is governed by the mechanical contact forces, pore water pressure, and the long-range physico-chemical forces.

The interparticle repulsion and attraction pressures are more important in fine grained soils than other granular soils, especially the ones with high specific surface (e.g. montmorillonite). Accordingly, the difference between the intergranular pressure and the conventional mechanical effective stress is the interparticle attractive minus repulsive stresses (Santamarina and Fam, 1995). As commonly known, a dispersed fabric has particles with minimal particle-particle relative inclination, while flocculated fabric particles form a honeycomb structure with larger particle-particle relative inclination. Eq. (1) suggests that a stronger van der Waals attraction and the weaker double layer repulsion result in a higher true effective stress. Since in non-expansive clays such as kaolinite van der Waals attraction is more dominant than double layer repulsion, then the fabric with the stronger van der Waals attraction results in a stronger specimen. Therefore, a dispersed fabric with a majority of particles parallel to each other is stronger, since van der Waals attraction is maximized when particles are parallel to each other (Jaradat and Abdelaziz, 2019). This is not the case for a flocculated fabric where particles are randomly oriented with a dominant edge-to-face contact.

CONCLUSIONS

The drained shear strength behavior of saturated clays was studied for different fabrics, utilizing a discrete element model developed for cohesive soils. The long-range physico-chemical forces existing in cohesive soils were considered and implemented in the model. To reduce the computational cost, simplified linear physico-chemical interactions were used instead of the non-linear actual interaction. The numerical model was validated against experimental lab test on saturated kaolinite. The impact of specimen fabric was studied by numerically shearing different kaolinite samples prepared at different fabric. It was shown that a dispersed normally consolidated fabric is stronger than a flocculated one, a behavior than was explained in light of the effective stress concept.

ACKNOWLEDGMENTS

This study was sponsored by the Army Research Office and was accomplished under Grant Numbers W911NF-16-1-0336, W911NF-18-1-0068 and W911NF-20-1-0238. The views and conclusions contained in this document are those of the authors and should not be interpreted as representing the official policies, either expressed or implied, of the Army Research Office or the U.S. Government.

REFERENCES

- Anandarajah, A., and Chen, J. (1994). "Double Layer Repulsive Force between Two Inclined Platy Particles According to the Gouy-Chapman Theory." *J. Colloid Inter. Sci.*, 68(1), 111-117.
- Anandarajah, A., and Chen, J. (1997). "Van der Waal Attractive Force Between Clay Particles in Water and Contaminants." *Soils Found.*, 37(2), 27-37.
- Chapman, D. L. (1913). "a contribution to the theory of electrocapilarity." *Philos. mag.*, 25(6), 475-481.
- Cundall, P. A., and Strack, O. D. L. (1979). "A discrete numerical model for granular assemblies." *Géotechnique*, 29(1), 47-65.
- Darbari, Z., Jaradat, K. A., and Abdelaziz, S. L. (2017). "Heating-freezing effects on the pore size distribution of a kaolinite clay." *Env. Earth Sci.*, 76(20), 713.
- Gouy, G. (1910). "Sur la constitution de la charge électrique à la surface d'un électrolyte." *Annuaire phys. (Paris)*, 9(1), 457-468.
- Iwashita, K., and Oda, M. (1999). *Mechanics of granular materials: an introduction*. CRC press.
- Jaradat, K. A., Darbari, Z., Elbakhshwan, M., Abdelaziz, S. L., Gill, S. K., Dooryhee, E., and Ecker, L. E. 2017. "Heating-freezing effects on the orientation of kaolin clay particles." *Appl. Clay Sci.*, 150, 163-174.
- Jaradat, K. A., and Abdelaziz, S. L. (2020). "Impact of Particle Size Distribution on Drained Shearing Response of Saturated Clays Using Discrete Element Method." In *Geo-Congress 2020: Modeling, Geomaterials, and Site Characterization*, ASCE, Reston, VA, 302-310.
- Jaradat, K. A., and Abdelaziz, S. L. (2019). "On the Use of Discrete element Method for Multi-Scale Assessment of Clay Behavior." *Comp. Geotech.*, 112(1), 329-341.
- Jaradat, K. A., and Abdelaziz, S. L. (2020). "Thermomechanical Triaxial Cell for Rate-Controlled Heating-Cooling Cycles." *Geotech. Test. J.*, 43(4).

- London, Z. (1937). "The general theory of molecular forces." *T. Faraday Soc.*, 33 (1), 8-26.
- Mitchell, J. K., and Soga, K. (2005). *Fundamentals of Soil Behavior*, Hoboken, NJ, John Wiley & Sons, Inc., 592 p.
- Prashant, A., and Penumadu, D. (2007). "Effect of microfabric on mechanical behavior of kaolin clay using cubical true triaxial testing." *J. Geotech. Geoenviron.*, 133(4), 433-444.
- PFC2D. 2019. *Particle flow code in two-dimensions*. Itasca Consulting Group,. 6.0 ed. Minneapolis, USA.
- Potts, D., and Zdravkovic, L. (1999). *Finite element analysis in geotechnical engineering: theory*. Thomas Telford.
- Santamarina, J. C., and Fam, M. (1995). "Changes in dielectric permittivity and shear wave velocity during concentration diffusion." *Can. Geotech. J.*, 32(4), 647-659.
- Van Olphen, H. (1977). *An introduction to clay colloid chemistry*, New York, 318 p., John Wiley & Sons, Inc.
- Yao, M., and Anandarajah, A. (2003). "Three-dimensional discrete element method of analysis of clays." *J. Eng. Mech.*, 129(6), 585-596.
- Yimsiri, S., and Soga, K. (2010). "DEM analysis of soil fabric effects on behaviour of sand." *Géotechnique*, 60(6), 483-495.
- Zeinali, S. M., and Abdelaziz, S. L. (2020a). "Freezing-Thawing on Saturated Clay Microstructure." In *Geo-Congress 2020: Geo-Systems, Sustainability, Geoenvironmental Engineering, and Unsaturated Soil Mechanics*, ASCE, Reston, VA, 40-48.
- Zeinali, S. M., and Abdelaziz, S. L. (2020b). "Effect of Heating Rate on Thermally Induced Pore Water Pressures and Volume Change of Saturated Soils" In *Geo-Congress 2020: Geo-Systems, Sustainability, Geoenvironmental Engineering, and Unsaturated Soil Mechanics*, ASCE, Reston, VA, 31-39.

Numerical Modelling of Bamboo Geogrid Reinforced Fly Ash Walls under Applied Uniform Loads

A. W. Mekonnen¹ and J. N. Mandal²

¹Assistant Professor, Dept. of Civil Engineering, Axum Institute of Technology, Axum, Tigray, Ethiopia. Email: abefikr@gmail.com

²Professor, Dept. of Civil Engineering, Indian Institute of Technology Bombay, Powai, Mumbai, India. Email: cejnm@civil.iitb.ac.in

ABSTRACT

This paper presents a numerical modeling to simulate the response of the experimental model studies conducted on bamboo geogrid reinforced fly ash walls under applied uniform load. Fly ash is a nonplastic and cohesionless material that has been considered as a waste, and it is a major concern for countries like India related to shortage of land for its disposal. In this regard, an attempt has been made for proper utilization of fly ash in a massive amount in the field of geotechnical engineering. The present study proposes fly ash as an alternative material to conventional soils to retaining wall applications as a backfill, and bamboo geogrid as a reinforcement. A series of experiments on reinforced fly ash model walls that comprise bamboo geogrid as a reinforcement under applied uniform loads has been conducted. The deformation behavior of the reinforced fly ash walls was studied systematically by considering a vertical spacing and varying the reinforcement length from 0.35 to 0.85 times the height of the model wall (H). The bamboo geogrids were placed in the testing tank in five layers in the form of bamboo geogrid strips. It was observed that the inclusion of bamboo geogrid strips improved the overall performance of the wall due to the confinement effect of the bamboo geogrid strips utilized as a reinforcement as compared to the unreinforced cases. In addition to that, as the length of reinforcement increases from 0.35 H to 0.85 H, the failure surcharge pressure and the facing deformation increase. However, for a particular surcharge load, increasing the reinforcement length decreases the facing deformation. This is attributed to the ability of longer reinforcements in load transfer mechanism and redistribution of the stresses in a wider area. Plaxis 3D has been used for the numerical simulation of the model experiments. The fly ash was modeled as linear elastic perfectly plastic material with a Mohr-Coulomb failure criterion, and the bamboo geogrid was modeled as an elasto-plastic material. Plaxis 3D overpredicts the horizontal wall movement, especially for longer reinforcements. However, it predicts the normalized settlement versus normalized failure surcharge pressure quite accurately.

Keywords: Fly Ash; Bamboo Geogrids; Plaxis 3D; Retaining Walls; Backfill.

INTRODUCTION

The rapid growth of urbanization and industry globally creates the need for a number of advanced power plant installations to fulfill the demand for electricity. As a result, a generation of fly ash is increasing at an alarming rate and its production exceeds its utilization (Dhadse et al. 2008). For example, the future production of fly ash will reach 600 million tons by the year 2031/2032 in India (Chatterjee 2011). Therefore, a huge amount of fly ash has to be stored and

causes environmental problems and ecological imbalance (Meegoda et al. 2011; Babu and Jaladurgam 2014). For example, in India, approximately 113 million square meters (m^2) agricultural land is covered by wet fly ash in ponds (Ahmaruzzaman 2010). Disposal of fly ash in an environmentally suitable way is a problem.

Generally, MSE walls have several advantages compared to conventional reinforced concrete and concrete gravity retaining walls. Cost-effectiveness, tolerant to deformation, less site preparation, technically feasible to heights of more than 25 meters and so on (Elias *et al.* 2001). In addition to that, they enable the soil to retain itself and surcharge loads using tensile reinforcement and facing elements (Xie and Leshinchsky 2015). Many experimental and numerical studies on reinforced soil walls have been conducted by several researchers in the past (for example, Ling et al. (2000), Ling and Leshchinsky (2003), Hatami and Bathurst (2006), Yang et al. (2009), Rathan Lal and Mandal (2014a), Kandolkar and Mandal (2016), Mekonnen and Mandal (2017), Mekonnen and Mandal (2018a)). Limited researches related to fly ash application in retaining walls (Rathan Lal and Mandal 2014a) and bamboo geogrid as a reinforcement in improvements of soft ground conditions are available (Dutta and Mandal 2015; Hegde and Sitharam 2015). Whereas, Feasibility study on fly ash and bamboo geogrid for retaining wall application was reported by Mekonnen and Mandal (2018b).

From the reviewed literature, it is clear that very limited research is get published using bamboo geogrid and fly ash as a geo-material. The experimental work has been conducted on bamboo geogrid reinforced fly ash walls under applied uniform load. This research is aimed to validate the potential of Plaxis 3D software to simulate the response of bamboo geogrid reinforced fly ash walls under applied uniform load in the laboratory. This research focuses on the study of the failure surcharge pressure, the backfill settlement, and the horizontal displacement of the facing.

MATERIALS USED FOR THE EXPERIMENT

The model experimental works have been conducted in a tank of 700 mm length, 340 mm width, and 550 mm height as shown in figure 1. The thickness and the contact area of the loading plate used are 10 mm and 330 mm x 540 mm respectively. The tank was made of steel and it also was manufactured with a transparent Perspex sheet for visual inspection of failure during loading stages. The test setup consisted of a 100-kN capacity reaction frame where a 20-kN capacity motor and a 50-kN capacity load cell were attached with. After removing the temporary supporter (plywood), four Linear Variable Differential Transducers (LVDTs) were securely fixed with the rear side of the tank. The movable spindles were facing along the centreline of the facia (concrete panels) in the direction of the tank height at a spacing of 100 mm. The vertical deformation/settlement was recorded by two LVDTs which were fixed at steel rods that ran at the top of the tank and securely welded with the posts of the reaction frame and the movable spindles facing perpendicular to the top surface of the load plate at a distance of $0.28b$ (b is the width of the loading plate) and $0.74b$ far from the facing. For each load increment, the two LVDTs measure the backfill settlement, and the four LVDTs measure the facing displacements until failure has occurred. Failure was considered when surcharge load was observed decreasing while the displacement of the facing was increasing. In all cases of the model experiments, the load plate was uniformly pushed by a motorized hydraulic Jack into the fly ash at a constant rate of 2 mm/min. similar procedures were followed for all the tests to know the variations of the parameters of the reinforcement used in each model (Mekonnen and Mandal 2018a). The

experimental studies were conducted for reinforcement lengths (L_r) ranging from $0.35H$ (H is the wall height)- $0.85H$, with a $0.1 H$ interval, the vertical spacing (S_v) and the coverage ratio (R_c) used were $0.2H$ and 0.5 , respectively. The fly ash used as a backfill material in this study has been classified per ASTM C618-15, as class F. It generally has 44% of sand-sized particles, 50.78% of silt-sized particles, 2% of medium sand-sized particles, and 3.2% of clay-sized particles. The uniformity coefficient (C_u) and coefficient of curvature (C_c) of the fly ash are 10 and 1.17 respectively. Whereas, the specific gravity (G_s), the maximum dry density (MDD), and the optimum moisture content (OMC) of the fly ash are 2.1, 12.54 kN/m^3 and 20%, respectively. On the other hand, the reinforcement used was prepared by hand from bamboo strips. The bamboo geogrid which has been prepared from 1 mm strip thickness and 10 mm strip width has created 10 mm x 10 mm square openings. The pick tensile strength has been determined per ASTM D4595-11 and its value is 42.4 kN/m .

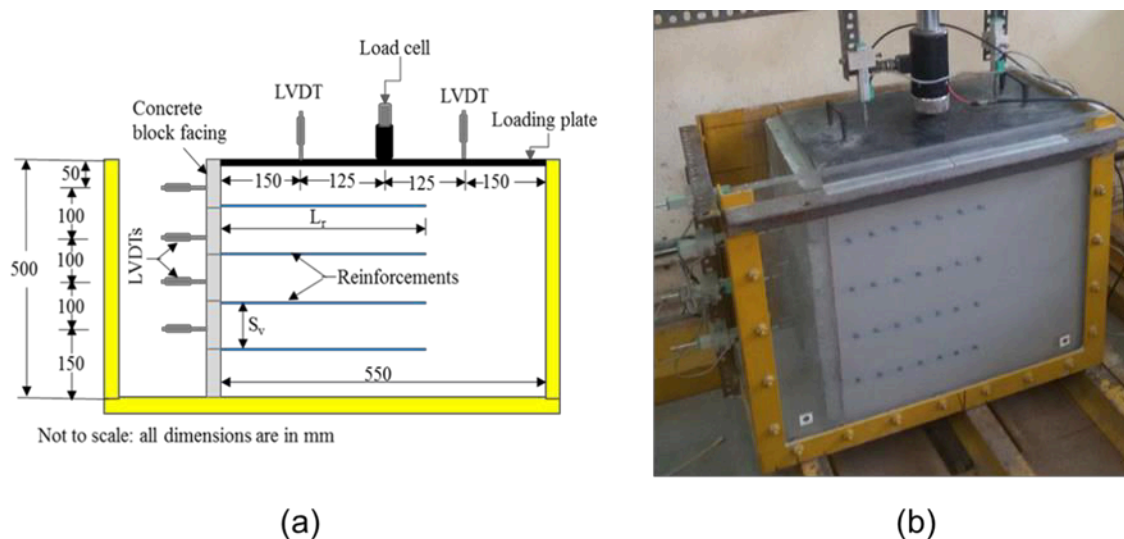


Figure 1. Bamboo geogrid reinforced fly ash wall subjected to applied uniform load: (a) line sketch (b) photograph.

SIMULATION OF THE MODEL WALLS BY FINITE ELEMENT METHODS

A series of three-dimensional finite element modeling and analyses on bamboo geogrid reinforced fly ash walls were executed to validate the laboratory model test results, and to know the deformation behavior within the bamboo geogrid fly ash wall system. Plaxis 3D finite element program was used for the analysis. Plaxis 3D is a commercially available finite element program that can handle a variety of geotechnical problems like tunnels, excavations, earth retaining structures, slopes, and so on. The geometry used in Plaxis 3D is similar to the laboratory model dimensions. Figure 2 shows the geometric and structural components of the model bamboo geogrid reinforced fly ash walls subjected to an applied uniform load. The finite element values obtained from Plaxis 3D, helped us to visualize failure patterns, to obtain backfill settlement and horizontal displacement results.